PCCP

Accepted Manuscript

ROYAL SOCIETY OF CHEMISTRY

www.rsc.org/pccp

Journal Name

RSCPublishing

ARTICLE

Structure and electronic properties of organo-halide lead perovskites: a combined IR-spectroscopy and ab-initio molecular dynamics investigation

Cite this: DOI: 10.1039/x0xx00000x

Received ooth January 2012,
Accepted ooth January 2012

DOI: 10.1039/x0xx00000x

www.rsc.org/

Edoardo Mosconi [a], Claudio Quarti [a*], Tanja Ivanovska [b], Giampiero Ruani [b*], Filippo De Angelis [a*]

Organo-halide lead perovskites are revolutionizing the photovoltaics scenario, with efficiencies exceeding 15%. The orientational dynamics disorder of the methylammonium cations (MA) is one of the most peculiar features of these materials. Here, we perform ab-initio molecular dynamics simulations and IR spectroscopic measurements on lead halide hybrid perovskites to elucidate the rotational motion of the MA cations in these systems and its effects on the structural and electronic properties of hybrid perovskites. In the investigated time frame, the MA cations do not show preferential orientations and are found to rotate within the inorganic framework on a timescale of a few ps. A variation of ±0.1-0.2 eV of the electronic properties with the ion dynamics is found, which increases by increasing the temperature.

1. Introduction

Organo-halide lead perovskites have raised the interest of the scientific community because of their unique properties, that make them highly attractive for opto-electronic applications.[1] In particular, in the field of photovoltaics, devices based on lead-halide perovskite showed a formidable and fast improvement[2-12], setting new records among organic and hybrid based solar cells and currently reaching a photo-to-current efficiency exceeding 15%.[11,12] In spite of the high efficiency of hybrid perovskite-based devices, the fundamental structural, optical and electronic properties of this class of materials are still in part unclear. If, on one side, the basic features of the crystalline and electronic structure of hybrid, lead halide perovskites have already been understood by means of both experimental[13,26] and theoretical tools[27-33], many open questions still remain about their detailed properties. A very intriguing issue of these materials deals with the orientation and the dynamics of the organic methylammonium (MA) cations inside the inorganic structure.[13-18] The presence of an ordered orientation of the MA cations in the low temperature phase of various hybrid perovskites have already been pointed out by several X-ray diffraction and DFT studies.[16-19] On the other hand, a fast rotational dynamics of the MA cations has been observed for the room temperature phase, with measured rotational relaxation and correlation time of 5.37 ps and 0.46 ps respectively, for the $CH_3NH_3PbI_3$ perovskite. It has also been suggested that in the cubic phase of lead-halide hybrid perovskites the MA cation rotates in an isotropic potential.[15] In spite of the fact that the organic component of lead-halide perovskite does not contribute directly to their energy band-gap[27], it has been pointed out that it can have important indirect effects on the structure[18,29] of these systems and also on their dielectric properties.[32]

Understanding the structural and electronic properties of the organo-halide lead perovskites, taking into consideration their intrinsic dynamical disorder, represents a mandatory step to gain a deeper comprehension of these systems. In this regard, ab-initio molecular dynamics represents a very powerful approach since it describes the electronic properties of these systems taking into account the dynamics of the ions in a coherent fashion. In addition, it considers thermal effects explicitly, allowing the simulation of the structural and electronic properties of the system of interest in conditions closer to the operative ones. In this work, we present the results of ab-initio Car-Parrinello molecular dynamics (CPMD) simulations on the $CH_3NH_3PbI_3$ organo-halide lead perovskite (here on $MAPbI_3$) and on the analogous $MAPbCl_3$ system, the former representing the prototype of hybrid lead halide perovskites for photovoltaic applications.[2,3,6,10,12] Very recently, the results from a CPMD simulation on the $CH_3NH_3PbI_3$

perovskite have been reported,[34] but this was mainly devoted to the study of the electronic properties of this material, not investigating its vibrational spectroscopic response. The vibrational response of these systems instead can provide very useful information on their dynamics, in particular, on the librational motion of the MA cations within the inorganic framework, that are expected in the low frequency range (below 500 cm^{-1}). In the present paper we also measured the IR spectrum of the related $CH_3NH_3PbI_{3-x}Cl_x$ perovskite at various temperatures, from 180 K to 293 K in the 30-500 cm^{-1} frequency range, and we compare these spectroscopic data with those obtained from the CPMD simulations on the $MAPbI_3$ perovskite. The Cl-doped perovskite has quite similar structural properties compared to $MAPbI_3$,[24] as recently reported. Its precise composition is not certain but a fraction of Cl-doping within 1% was proposed[24] and thus, due to the similarity of the two materials, we do not expect substantial variation in the IR spectroscopic features associated to MA cation dynamics. It is worth to mention that we are not interested here in the detailed assignment of the vibrational features of lead halide perovskites, that has been recently reported by some of us.[25] We rather wish to compare the results of our dynamics simulations to the spectroscopic IR data obtained in this study and with the other spectroscopic data available from the literature,[21,26] providing a potentially useful insight on the structure and on the dynamics of the MA cations in organo-halide lead perovskites.

Our study indicates that in the cubic phase of $MAPbI_3$ the MA cations have large orientational mobility and, most notably, that their motion is strongly coupled to that of the inorganic framework. In addition, the qualitatively good agreement of the simulated IR spectra at two different temperatures with the experimental spectra, demonstrates the importance of the orientational dynamics of the MA cations in the spectroscopic response of lead-halide hybrid perovskites. The variation of the electronic properties due to the atomic motion is also investigated, finding that nuclear dynamics can lead to energetic shifts of the order of few tenths of eVs.

2 Experimental and theoretical methods

2.1 Models and methods.

Car-Parrinello Molecular Dynamics (CPMD),[35] as implemented in the Quantum-Espresso package[36] is used in the present work. The structural model used for CPMD simulations is composed by a 2x2x2 cubic supercell of 8 $MAPbX_3$ (X=Cl and I) units, see Figure 1a, employing the experimental cell parameters (6.3288 and 5.6752 Å for X=I and Cl, respectively).[13] The $MAPbI_3$ perovskite is known to undergo phase transitions from the room temperature tetragonal to the high temperature cubic structure at 327 K, while $MAPbCl_3$ is cubic at room temperature.[13] Thus, the choice of the cubic framework in both X=I and Cl thus seems to be a good compromise to compare their structure and spectroscopic response in similar conditions. To avoid possible inconsistencies due to the temperature-induced phase transitions, we fixed the Pb atoms at their cubic sites. CPMD simulations were conducted at two temperatures, i.e. 268 K and at 319 K for X=I, and at 291 K for X=Cl, for a total simulation time of ~13 ps, after few ps of equilibration. We notice that at 268 K the $MAPbCl_3$ perovskite is in the stability conditions of the cubic phase. At 319 K instead, $MAPbI_3$ is very close to the tetragonal to cubic transition (327 K), while, at the opposite, the simulation of a cubic MAPbI3 at 268 K represents a hypothetical strongly undercooled cubic structure. Nevertheless, at the light of the very similar parameters of the pseudo-cubic lattice parameter (6.26 Å) with respect to the cubic one (6.33 Å), we expect that the assumption of a cubic structure at temperatures lower than the transition one does not introduce significant differences with respect to the real case, as demonstrated in the Section 3.1. To decouple the effect of the MA dynamics from that of the inorganic counterpart, we performed additional CPMD simulations with all the inorganic atoms fixed at their corresponding cubic sites and only the atoms of the MA cations were allowed to move (*Pb-I-fixed* model). If not otherwise stated, our results refer to the case with only the Pb atoms fixed. CPMD simulations have been carried out with an integration time step of 4 au, fictitious electronic mass of 400 au, and the real ionic masses. The PBE exchange-correlation functional[37] was used along with ultrasoft,[38] scalar relativistic pseudopotentials for all atoms. We used a cutoff of 25 and 200 Ry, respectively, for expansion of the electronic wavefunctions and charge density.

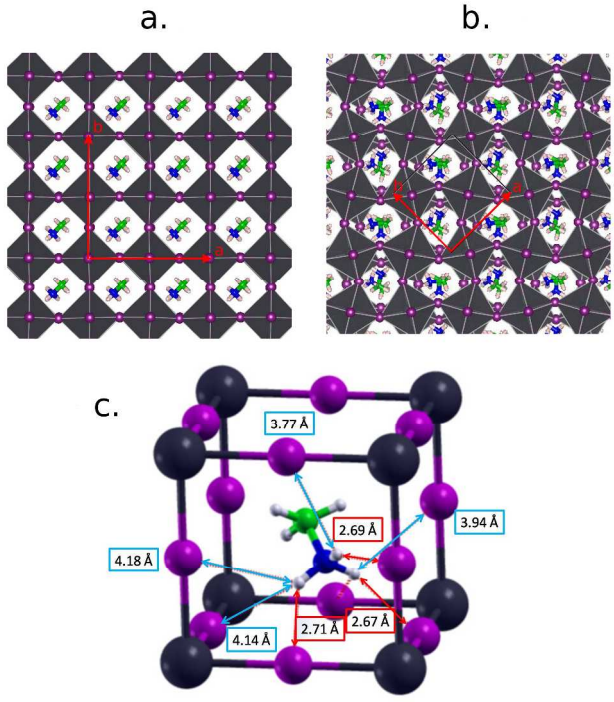

Figure 1. a) Cubic model and b) tetragonal model structures. Highlighted are the employed simulation cells. c) Starting orientation of the MA cation in the cubic phase.

We calculated the IR spectra of $MAPbI_3$ from the CPMD simulations using the relation between the IR intensity and the dipole autocorrelation function:[39]

$$I(\omega) = \frac{2\pi\beta\omega^2}{3cV}\int_{-\infty}^{+\infty} \mathrm{d}t\langle \mathbf{M}(t)\cdot\mathbf{M}(0)\rangle \exp(\mathrm{i}\omega t)$$

where the angular brackets indicate a statistical average of the correlation of the dipole moment **M** of the system.

For further comparison, we have also calculated the IR spectrum of the more stable tetragonal $MAPbI_3$ structure,[25,28] made by four $MAPbI_3$ units, Figure 1b, by a static phonon calculation on the relaxed (atomic and lattice) structure. The calculated cell parameters are 8.783 Å, 8.746 Å, and 12.699 Å, which are in good agreement (within 1%) with experimental data.[13] The phonon calculation has been carried out at the same level of theory of the CPMD simulations, namely with the PBE exchange-correlation functional, ultrasoft, scalar relativistic pseudopotentials and with a cutoff of 25 Ry and 200 Ry, respectively, for the wavefunction and for the density expansion. A 4x4x4 mesh for sampling the first Brillouin zone is used.[40]

2.2 Material synthesis and spectroscopic measurements

The material has been prepared according to the published procedure,[5] as follows: 24 ml of methylamine solution (33 wt% in absolute ethanol) was mixed with 100 ml of ethanol and 10 ml of 57% HI acid. The solution was stirred for 2 hours, then transferred to rotary evaporator and kept at 70°C until a crystalline powder formed. The crystalline powder was washed and recrystallized from ethanol and the formed methylammonium iodide was dried in a furnace at 60°C for 16 hours. The CH_3NH_3I and $PbCl_2$ were dissolved at a 3:1 molar ratio in N,N-Dimethylformamide to form a 40 wt% $MAPbI_{3-x}Cl_x$ perovskite precursor solution.[7] A 13±1 μm thick mixed halide perovskite film was deposited on 1 mm thick high density polyethylene (HDPE) substrate by spin coating under nitrogen atmosphere and annealed at 70°C for 45 min. After annealing a PMMA solution in chlorobenzene (Allresist 671.05) was spin coated on top of the film before exposing to air.

FAR IR absorption spectra were obtained by using a Bruker 113v FT-IR spectrometer at 2 cm^{-1} resolution averaging over 256 scans. In order to optimize the quality of the spectra in the Far IR spectral range we have investigated (30-500 cm^{-1}), at each temperature two spectra were collected by using two distinct mylar beamsplitters (12 μm for the spectral region below 200cm^{-1} and 3.5 μm above 200 cm^{-1}). As reference, a sample was prepared by spin coating directly the PMMA solution on top of a twin HDPE substrate. Temperature dependent measurements were performed mounting the sample on the cold finger (with a 6 mm aperture hole) of a flow cryostat with HDPE windows with the $MAPbI_{3-x}Cl_x$ in direct contact with the copper cold finger. The temperature was monitored by ITC4 Oxford temperature controller; in order to let the temperature stabilize, the IR measurements were performed 15 minutes after setting the designed temperature, ensuring that the variation was not larger than 1 K.

3. Results and Discussion

3.1 Structural properties.

In Figure 2 we report the radial distribution function (RDF) associated to the inorganic framework of $MAPbI_3$, obtained from the CPMD simulations at 268 K and 319 K, compared with the experimental RDF reported in Ref 21.

The theoretical RDF of the inorganic atoms of $MAPbI_3$ does not show substantial variations with the temperature. Moreover, the theoretical RDF in Figure 2 parallels very well the experimental data; in particular, the first two peaks at 3.20 and 4.45 Å are predicted in very good agreement in both position and broadening, indicating that both the average distances between inorganic ions and their variation due to the ion dynamics are correctly described by our simulation. The peak at ~6.3 Å is also in good agreement with the experiment, indicating that the information on the second coordination shell of the inorganic ions is correctly predicted. The very weak signal predicted at ~5.4 Å can be associated to that observed experimentally at ~5.6 Å (see Figure SI1, Supplementary Information). The absence of this signal in the RDF obtained for the *Pb-I-fixed* model (i.e. the model with Pb and I atoms fixed at their cubic sites) demonstrates that this weak signal arises from the displacement of the iodine atoms from their equilibrium position (see Figure SI2). The theoretical RDF slightly differs with respect to the experiment only at distances larger than 7 Å. The two signals predicted at 7 Å and at 7.7 Å are present also in the RDF of the *Pb-I-fixed* model (See Figure SI2), thus they are inherent in our cubic structure model. At the opposite, the RDF obtained by Choi et. al. on a tetragonal model reproduces the experimental RDF also above 7 Å.[21] It is thus clear that the differences between our theoretical RDF and the experimental one at large distances (>7 Å) must be addressed to the cubic model employed here.

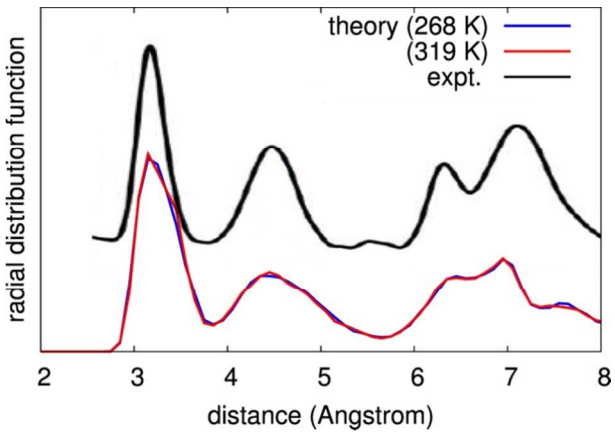

Figure 2. Radial distribution function (RDF) of the inorganic ions of $MAPbI_3$, obtained from the CPMD simulation carried out at the temperatures of 268 K (blue) and 319 K (red), compared with the experimental RDF from Ref 21 (black).

We have monitored the orientation of the MA ions during the CPMD simulations at different temperatures. As showed in Figure SI3-SI4, the MA cations do not assume preferred orientations but rather they explore almost all possible orientations inside the inorganic cage already at the lowest simulated temperature (268 K) and no evident modifications of the orientational dynamics take place at higher temperatures. These results confirm that in the cubic phase of hybrid lead-halide perovskites, the MA cation rotates in an isotropic potential, as pointed out in Ref 15. During the simulation, the MA cations accomplish at least one rotation along one of the reference axes (see Table SI1-SI2), providing a mean rotation time of the order of few ps (5.47 ps at 268 K, 4.52 at 319 K)†. These results agree quite well with the experimental estimation of the C-N rotational correlation time in $MAPbI_3$ of 0.46 ps[14] and with the relaxation process of the MA cations in $MAPbI_3$ of 5.47 ps.[13]†† During the simulations on the *Pb-I-fixed* model instead, the molecules remain in their original orientation (see Figure SI5-SI6), without rotating during the whole simulation time. These results demonstrate that the rotational dynamics of the MA cations is strongly coupled with the dynamics of the inorganic counterpart.

We previously showed [25] that the torsional vibrations of the MA cations, found between 200 and 300 cm^{-1}, could be strongly red-shifted by specific organic-inorganic interactions. Since the organic-inorganic interactions are mainly occurring through Coulomb and hydrogen-bonds interactions between the NH_3 groups of the MA cations and the electronegative iodine atoms,[18,27,28] we have analyzed the distance between the hydrogen atoms of the NH_3 group and the iodine atoms during the CPMD dynamics. In Figure 3, we report the H-I RDF at 268 K and at 319 K. This data clearly shows two maxima at about 2.65 Å and 4.10 Å, that correspond to the first and second H-I coordination (see Figure 1c), which does not change substantially with the simulation temperature. A similar situation is showed in the RDF of the *Pb-I-fixed* model, which shows sharper peaks due to reduced variety of configurations of the organic to inorganic interactions, confirming that the motion of the organic and of inorganic counterparts are strongly coupled (see Figure SI7).

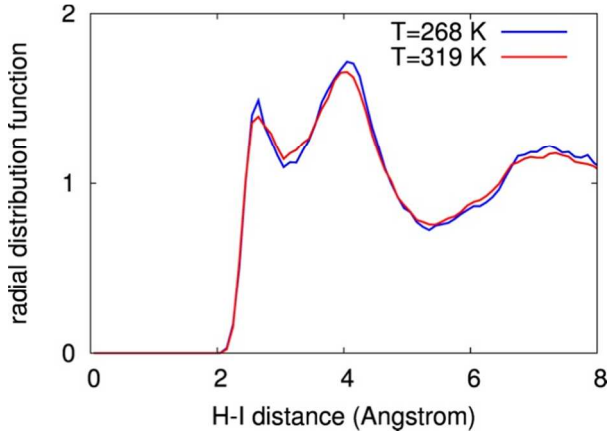

Figure 3. Radial distribution function for the iodines and the hydrogens of the NH_3 groups predicted by the CPMD simulations at 268 (blue) and 319 (red) K.

Note that the situation depicted by the CPMD simulations, where the first interaction shell extends from 2 Å to more than 2.5 Å, is more complex than that of the static models proposed in the literature.[19,28] In the static models based on the tetragonal structure of $MAPbI_3$,[28] the first coordination shell is composed by two H to I distances ~2.55 Å and a third one ~2.85 Å, providing a mean interaction distance of ~2.65 Å. Similarly, in the model obtained from X-ray diffraction for the orthorhombic structure of $MAPbI_3$ [19] the first coordination shell is composed by three H to I distances of ~2.55 Å.

Summarizing, the MA cations show a large orientational motion in the $MAPbI_3$ perovskite, which is strongly coupled with the motion of the inorganic structure. As a consequence of the rotational freedom of the MA cations, there is a large variety of organic-inorganic interactions in terms of relative configurations of the MA cations with respect to the inorganic cage. We anticipate that this rotational freedom should manifests itself with a specific spectroscopic marker in the vibrational IR spectrum of $MAPbI_3$, as discussed in the next Section.

3.2 IR Spectroscopy

In this Section, we investigate the structure of the $MAPbI_3$ with the vibrational IR spectroscopy. Useful information on the dynamics of the MA cations in hybrid lead halide perovskites are expected in the low frequency region, thus we recorded the experimental IR spectrum of the $MAPbI_{3-x}Cl_x$ perovskite in the frequency region from 30-500 cm^{-1} at various temperatures and we compare it with the results from our theoretical simulations on the $MAPbI_3$.

The vibrational Raman spectrum of $MAPbI_3$ showed a broad and not resolved signal between 200-300 cm^{-1},[25] which was not paralleled in the static phonon calculations. We proposed that the frequency of the torsional vibration of the MA cations could easily red-shift from 400 cm^{-1} to the region between 200-300 cm^{-1} because of the specific interactions of the MA cations with the inorganic counterpart and thus we have proposed this signal as an important marker of the organic-

inorganic interactions. In Figure 4a, the experimental IR spectrum of $MAPbI_{3-x}Cl_x$ is reported at various temperature between 180 K and 293 K. Most notably, the measured IR spectra also show a broad band between 200-300 cm^{-1}. This band clearly shifts to lower frequencies and broadens with increasing temperature (see inset of Figure 4a). The results from the phonon calculation on the tetragonal $MAPbI_3$ model[29] and from the CPMD simulations on the cubic model are reported respectively in Figure 4b and Figure 4c. The convergence of the IR spectra from the CPMD simulations with respect to the simulation time has been carefully checked (see Figure SI8 and SI9). The signal found experimentally between 200-300 cm^{-1} is clearly absent in the static phonon calculation. Only four weak signals from the torsional mode of the MA cations are present at 271, 301, 307 and 309 cm^{-1} (see the inset in Figure 4b). At the opposite, the IR spectrum predicted from the CPMD simulations on the cubic model at finite temperature predicts a broad signal at 200-300 cm^{-1}. Broadening of the IR bands is associated to fast rotational motion of MA cations, as observed in other systems where molecules are free to rotate in the solid state like plastic crystals of C_{60}.[41] Most notably, our simulations also reproduce the experimental red-shift of this band with the temperature (see Figure 4c).

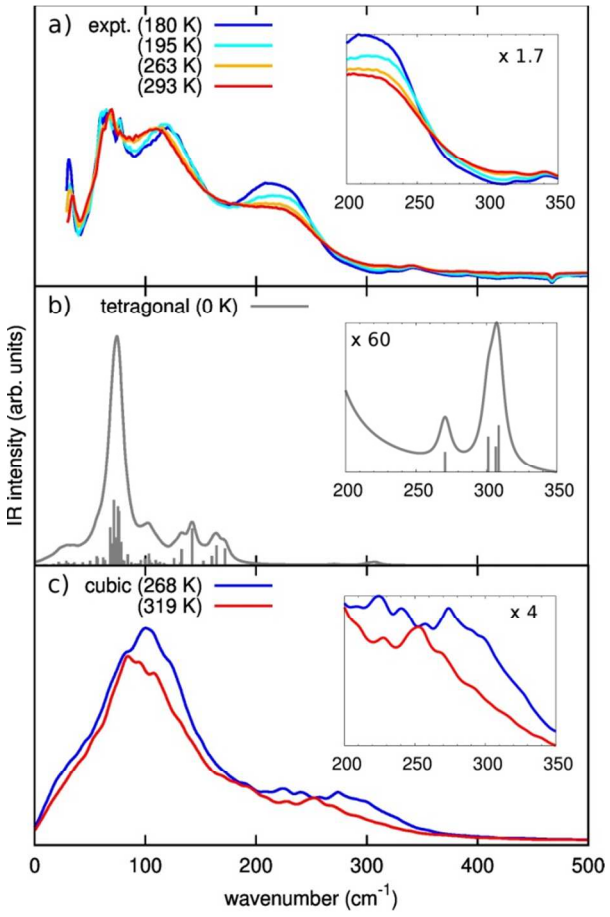

Figure 4. a) Experimental IR spectrum of $MAPbI_{3-x}Cl_x$ perovskite recorded at 180 K, 193 K, 263 K and 293 K; b) theoretical IR spectrum from the static phonon calculation on the tetragonal structure (proposed in Ref 28 for the $MAPbI_3$ perovskite); c) theoretical IR spectrum from the CPMD simulations at 268 K and 319 K. In the Insets, we report the detail of the experimental and theoretical spectra in the 200-350 cm^{-1} frequency region, with the respective intensity magnification factor.

The better performance of the CPMD simulations on the static calculation to predict the IR spectrum of the hybrid lead halide perovskites in the 200-300 cm^{-1} frequency region should be referred to the different description of the structure of these systems in terms of orientational dynamics of the MA cations and in terms of the organic-inorganic interactions, as pointed out in the previous Section. This is consistent with the analysis in Ref. 25, where it was shown that the specific organic-inorganic interactions play a crucial role in the frequency of the torsional vibration of the $MAPbI_3$. Summarizing, the present analysis demonstrates the importance of the orientational dynamics of the MA cations in $MAPbI_3$ for the correct prediction of the vibrational spectroscopic response of this material.

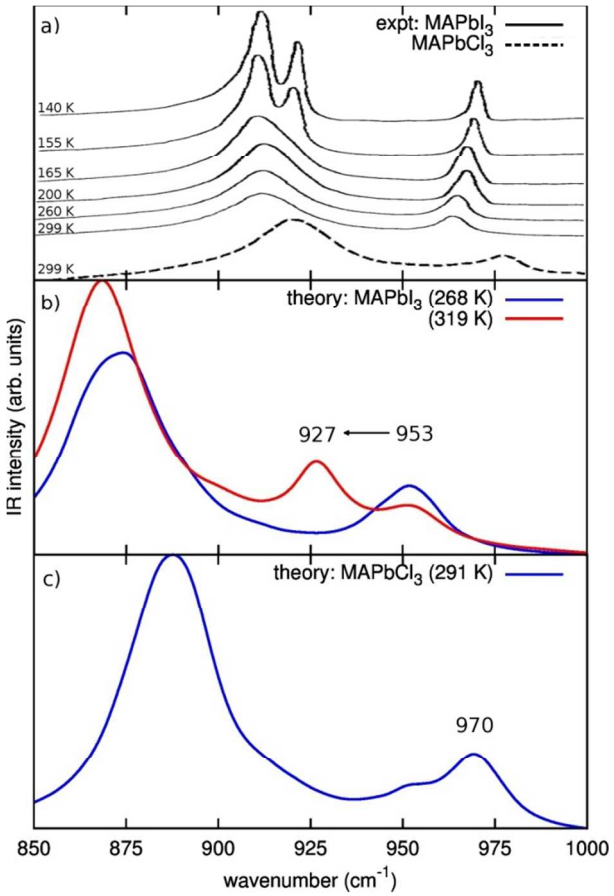

Figure 5. Experimental and theoretical IR spectrum of $MAPbI_3$ and of $MAPbCl_3$ perovskites in the region between 850-1000 cm^{-1}. a) experimental IR spectrum of $MAPbCl_3$ at 299 K and that of $MAPbI_3$ at various temperatures; b) theoretical spectrum from CPMD of $MAPbI_3$ at 268 and at 319 K; c) the theoretical spectrum from CPMD of $MAPbCl_3$ at 291 K. Experimental data taken from Ref 26.

To further explore the effect of the intermolecular interactions on the IR spectra of the investigated systems, we compare in Figure 5 the CPMD-simulated IR spectra of $MAPbI_3$ and $MAPbCl_3$ with the experimental IR spectra in the 850-1000 cm^{-1} frequency region.[26] The experimental spectra in this region have been reported by Onoda-Yamamuro et al.,[26] who assigned the low and the high frequency band to the rocking and to the CN stretching vibrations of the MA cations, respectively. As shown in Figure 5, the CPMD simulation reproduce the CN stretching signal in very good agreement with experiments. The CN stretching of $MAPbI_3$ is predicted at 953 cm^{-1} at 268 K, compared to ~965 cm^{-1} found experimentally at similar temperature. The CN stretching of $MAPbCl_3$ is predicted at 970 cm^{-1}, compared with 980 cm^{-1} at similar temperature. Considering the dependence of the frequency of this vibration on the temperature and the presence of hydrogen bonds, which typically affect the vibrational frequency of organic systems, the present agreement is quite satisfactorily. Our results also nicely reproduce the red-shift of about 20 cm^{-1} of the CN band from $MAPbCl_3$ to $MAPbI_3$ perovskite. The calculated shift is due to the interaction of the MA cation with the halogen atom (Cl or I), highlighting the importance of organic-inorganic interactions in this class of systems. We also notice that we significantly underestimate the frequency of the rocking band of the MA cations, though we still predict the relative position of this band for $MAPbCl_3$ with respect to $MAPbI_3$. In our opinion, this fact should be addressed to a well known limitation of the CPMD method. It has been already pointed out in fact that the choice of large values for the electron fictitious mass can lead to correlation between the nuclei spectra and the spectrum of the fictitious electronic degrees of freedom.[39] In a previous work by Gaigeot et. Al., an underestimation of few tens of cm^{-1} of the rocking band of liquid methanol by CPMD simulation with respect to the experiment was found.[42] As last note, an evident red-shift of the CN stretching band with increasing the temperature is observed experimentally and this feature is very well reproduced by our CPMD calculations. The predicted shift is clearly overestimated by theoretical calculations but it is worth to note that our CPMD simulations explore higher temperatures than those reported in the experiment.

3.3 Electronic properties.

To investigate the effect of the ion dynamics on the electronic properties of the $MAPbI_3$ perovskite, we have analyzed the evolution of the HOMO energy during the CPMD simulations.

We recall that the $MAPbI_3$ valence band, thus the HOMO, is mainly made by I orbitals, while the conduction band is mainly made by Pb states.[27,29] We expect the band gap to show somehow comparable energy oscillations to those observed for the HOMO orbital energy. It is worth to note that the dependence of the variation of the electronic properties from molecular dynamics simulations should be checked with respect to both the size of the model and the simulation time. Dealing with the first point, we are quite confident of the reliability of our data. In fact, the RDF of the inorganic structure in Figure 2 demonstrates that our simulations describe accurately the dynamics of the ions within a distance of more than 1 cubic unit and, since the HOMO energy is expected to vary with the dynamics of the inorganic atoms, we consider our results to be reliable. The dependence of the HOMO energy variation with the simulation time instead has been carefully verified for the CPMD simulations at 268 K and 319 K (See Figure SI10 and SI11). In Figure 6 we report the evolution of the energy of the HOMO during the CPMD simulation at 319 K.

A statistical analysis of the HOMO energy for all the CPMD simulations has been carried out and its main results are summarized in Table 1. The distribution of the HOMO energies are well approximated by gaussian distributions (See Figure SI12-SI13). There is an evident increase in the RMS of the HOMO energy with the temperature, in line with the expected larger displacement of the ions at higher temperature. It is also worth to note that the RMS and mix/max HOMO values in the simulations on the *Pb-I-fixed* model are 5-7 times smaller than the data in Table 1 (See Figures SI12-SI15). This result is perfectly expected, because of the main contributions from the inorganic iodine atoms on the HOMO band gap[27] and thus the constrain on the dynamics of these ions in the *Pb-I-fixed* model obviously results in less spread energy values of the HOMO orbital.

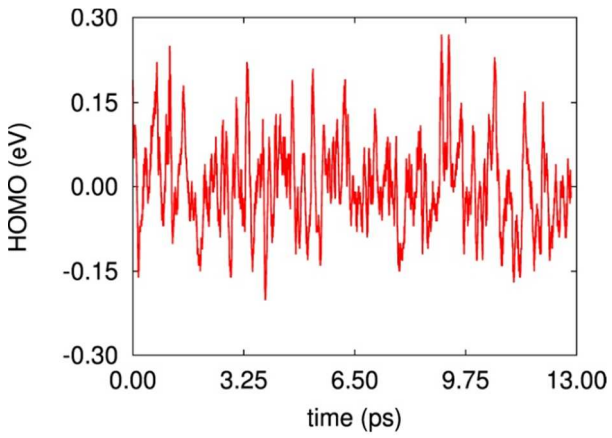

Figure 6. Energy variation of the HOMO orbital during the CPMD simulation of $MAPbI_3$ at 319 K. The average HOMO energy has been set to 0.

The most relevant feature that emerges from Table 1 is that the variation of the electronic properties of $MAPbI_3$ is of the order of few tenths of eV. This means that 95% of the values assumed by the HOMO fall in the range of about 0.22 eV and 0.31 eV, respectively at 268 K and at 319 K, which is comparable to the variation of the electronic properties typically found for organic semiconductors and dye-sensitized interfaces.[43,44,45]

Table 1. Average, root mean square (RMS), maximum and minimum value assumed by the HOMO orbital during the CPMD simulations at the various temperatures for the cubic model.

temperature (K)	RMS (eV)	max – min (eV)
268	$5.39\ 10^{-2}$	0.34
319	$7.80\ 10^{-2}$	0.47

Conclusions

Organo-halide lead perovskites represent one the most interesting innovation in the field of new materials for photovoltaic applications, because of their unique properties. Nevertheless, there are still many open questions on their structural properties. Several works in the literature pointed out the extremely fast dynamics of the methylammonium (MA) cations in the organo-halide lead $CH_3NH_3PbI_3$ ($MAPbI_3$) perovskite[13,14] and some authors have demonstrated that the organic counterparts have important effects on both the structure[29] and optical properties[32] of these materials. In this work we have carried out ab-initio Car-Parrinello molecular dynamics simulations on the $MAPbI_3$ perovskite, in order to investigate on the dynamics of the MA cations in this hybrid perovskite. In addition, we have measured the IR spectrum of the $MAPbI_{3-x}Cl_x$ perovskite in the low frequency region, where the libration motions of the MA cations are expected. The results from these simulations are in good agreement with the available experimental data. A very fast rotational motion of the organic cation inside the inorganic structure is found, with rotational times of the order of 4-6 ps. Such rotational motion is already present at relatively low temperature (268 K) in the cubic phase and it is strongly correlated to the dynamics of the inorganic ions. The strong coupling of the dynamics of the organic ions and of the inorganic counterpart results in a clear spectroscopic marker in the broad and not defined band between 200-300 cm^{-1} in the IR spectrum of $MAPbI_3$. As a last result, the variation of the electronic properties of this material close to room temperature, due to the ion dynamics, is estimated in the order of a few tenths of eV, which is comparable with the variations of the electronic properties in organic semiconductors.

Acknowledgements

The research leading to these results has received funding from the European Union Seventh Framework Programme [FP7/2007-2013] under grant agreement n° 604032 of the MESO project.

Notes and references

[a] Computational Laboratory for Hybrid/Organic Photovoltaics (CLHYO), CNR-ISTM, I-06123, Perugia, Italy

[b] Istituto per lo Studio dei Materiali Nanostrutturati, Consiglio Nazionale delle Ricerche (CNR-ISMN), Via Gobetti 101, 40129 Bologna, Italy.

*E-mail: claudio@thch.unipg.it, g.ruani@bo.ismn.cnr.it, filippo@thch.unipg.it

† These numbers do not provide a highly accurate estimation of the full rotation times because of the short time simulation with respect to the time scale of the rotations. To get accurate rotational time, much longer molecular dynamics simulations are needed but the present estimation provides at the same time an accurate order-of-magnitude prediction.

†† Both the "relaxation time" and the "correlation time" are indirect measures of the time required by the methylammonium (MA) cations to accomplish a rotation. In particular, the "relaxation time" from Ref. 13 is the response of the material to an electromagnetic field and it has been associated to the MA cation mobility. The "correlation time" from ref. 14 is a measure of the time required by the MA cation to accomplish a rotation of one radiant; in the latter case, a rough estimation of the time required by the MA to accomplish a full rotation of 360 degrees in MAPbI3 is $\geq$ 2.89 ps. Thus, the averaged rotational times obtained by our CPMD simulations (5.47 ps and 4.52 ps respectively at 268 K and at 319 K) show a quite good agreement with the experimental data available.

Electronic Supplementary Information (ESI) available: magnification of the RDF of the inorganic framework in the region between 4 and 6 Å (Figure SI1). Radial distribution function of the inorganic framework computed on the *Pb-I-fixed* model (Figure SI2). Orientation of the MA cations during the simulations at 268 K, 319 K (respectively Figure SI3, SI4) and for the *Pb-I-fixed* model during the simulations at 350 K and 420 K (respectively Figure SI5, SI6). Number of rotations of the MA cations along the three reference axis in the cubic model during the simulations at 268 K, 319 K (respectively Table SI1, SI2). Radial distribution function of the distance between iodines and hydrogen atoms of the NH_3 group computed on the *Pb-I-fixed* model (Figure SI7). Convergence of the IR spectra from the CPMD simulations at 268 K and 319 K with respect to the simulation time (Figure SI8, SI9). Convergence of the spreading of the HOMO energies from the CPMD simulations at 268 K and 319 K with respect to the simulation time (Figure SI10, SI11). Distribution of the HOMO energy of the cubic model during the simulations at 268 K, 319 K (respectively Figure SI12, SI13) and of the *Pb-I-fixed* model during the simulations at 350 K, 420 K (respectively Figure SI14, SI15). See DOI: 10.1039/b000000x/

1 D. B. Mitzi, Solution-processed Inorganic Semiconductors. *J. Mater. Chem.* 2004, 14, 2355-2365.

2 J. H. Im, C. R. Lee, J. W. Lee, S. W. Park and N. G. Park, 6.5% Efficient Perovskite Quantum-Dot-Sensitized Solar Cell. *Nanoscale* 2011, **3**, 4088–4093.

3 A. Kojima, K. Teshima, Y. Shirai and T. Miyasaka, Organometal Halide Perovskites as Visible-Light Sensitizers for Photovoltaic Cells. *J. Am. Chem. Soc.* 2009, **131**, 6050–6051.

4 I. Chung, B. Lee, J. He, R. P. H. Chang and M. Kanatzidis, All-Solid-State Dye-Sensitized Solar Cells With High Efficiency. *Nature* 2012, **485**, 486-489.

5 M. M. Lee, J. Teuscher, T. Miyasaka, T. N. Murakami and H. J. Snaith, Efficient Hybrid Solar Cells Based on Meso-Superstructured Organometal Halide Perovskites. *Science* 2012, **338**, 463-467.

6 L. Etgar, P. Gao, Z. Xue, Q. Peng, A. K. Chandiran, B. Liu, Md. K. Nazeeruddin, and M. Grätzel, Mesoscopic $CH_3NH_3PbI_3/TiO_2$ Heterojunction Solar Cells. *J. Am. Chem. Soc.* 2012, **134**, 17396−17399.

7 J. M. Ball, M. M. Lee, A. Hey and H. J. Snaith, Low-temperature processed meso-superstructured to thin-film perovskite solar cells. *Energy Environ. Sci*. 2013, **6**, 1739-1743.

8 E. J. W. Crossland, N. Noel, V. Sivaram, T. Leijtens, J. A. Alexander-Webber and H. J. Snaith, Mesoporous TiO_2 Single Crystals Delivering Enhanced Mobility And Optoelectronic Device Performance. *Nature* 2013, **495**, 215-219.

9 A. Abrusci, S. D. Stranks, P. Docampo, H.L. Yip, A. K. J. Jen and H. J. Snaith, High-Performance Perovskite-Polymer Hybrid Solar Cells via Electronic Coupling with Fullerene Monolayers. *Nano Lett.* 2013, **13**, 3124−3128.

10 J. H. Heo, S. H. Im, J. H. Noh, T. N. Mandal, C. S. Lim, J. A. Chang, Y. H. Lee, H. J. Kim, A. Sarkar, Md. K. Nazeeruddin, M. Grätzel and S. I. Seok, Efficient Inorganic–Organic Hybrid Heterojunction Solar Cells Containing Perovskite Compound and Polymeric Hole Conductors. *Nature Photon.* **2013**, *7*, 486-491.

11 M. Liu, M. B. Johnston and H. J. Snaith, Efficient Planar Heterojunction Perovskite Solar Cells By Vapour Deposition. *Nature* 2013, **501**, 395–398.

12 J. Burschka, N. Pellet, S. J. Moon, R. Humphry-Baker, G. Peng, Md. K. Nazeeruddin, M. Grätzel, Sequential Deposition as a Route to High-Performance Perovskite-Sensitized Solar Cells. *Nature* 2013, **499**, 316-319.

13 A. Poglitsch and D. Weber, Dynamic Disorder in Methylammoniumtrihalogenoplumbates (II) Observed by Millimeterwave Spectroscopy. *J. Chem. Phys. 1987,* **87***,* 6373-6378.

14 R. E. Wasylishen, O. Knop, J. B. Macdonald Cation Rotation in Methylammonium Lead Halides, *Solid State Commun.* 1985, **56**, 581-582.

15 O. Knop, R. R. Wasylishen, M. A. White, T. S. Cameron and M. J. M. Van Oort, Alkylammonium lead halides. Part 2. $CH_3NH_3PbX_3$ (X=C1, Br, I) perovskites: cuboctahedral halide cages with isotropic cation reorientation. *Can. J.Chem.* 1990, **68**, 412-422.

16 I. P. Swainson, R. P. Hammond, C. Soullière, O. Knop and W. Massa, Phase transitions in the perovskite methylammonium lead bromide, $CH_3ND_3PbBr_3$. *J. Solid State Chem.* 2003, **176**, 97-104.

17 L. Chi, I. Swainson, L. Cranswick, J. H. Her, P. Stephens and O. Knop, The ordered phase of methylammonium lead chloride $CH_3ND_3PbCl_3$. *J. Solid State Chem.* 178, **2005**, 1376-1385.

18 I. Swainson, L. Chi, J. H. Her, L. Cranswick, P. Stephens, B. Winkler, D. J. Wilson and V. Milman, Orientational ordering, tilting and lone-pair activity in the perovskite methylammonium tin bromide, $CH_3NH_3SnBr_3$. *Acta Cryst.* B66, **2010**, 422-429.

19 T. Baikie, Y. Fang, J. M. Kadro, M. Schreyer, F. Wei, S. G. Mhaisalkar, M. Grätzel, and T. J. White, Synthesis and Crystal Chemistry of the Hybrid Perovskite $(CH_3NH_3)PbI_3$ for Solid-State Sensitised Solar Cell Applications. *J. Mater. Chem. A* 2013, **1**, 5628–5641.

20 C. C. Stoumpos, C. D. Malliakas, and M. G. Kanatzidis, Semiconducting Tin and Lead Iodide Perovskites with Organic Cations: Phase Transitions, High Mobilities, and Near-Infrared Photoluminescent Properties. *Inorg. Chem.* 2013, **52**, 9019−9038.

21 J. J. Choi, X. Yang, Z. M. Norman, S. J. L. Billinge and J. S. Owen, Structure of Methylammonium Lead Iodide Within Mesoporous Titanium Dioxide: Active Material in High Performance Perovskite Solar Cells, *Nano Lett.* 2014, **14**, 127-133.

22 S. D. Stranks, G. E. Eperon, G. Grancini, C. Menelaou, M. J. P. Alcocer, T. Leijtens, L. M. Herz, A. Petrozza and H. J. Snaith, Electron-Hole Diffusion Lengths Exceeding 1 Micrometer in an Organometal Trihalide Perovskite Absorber. *Science* 2013, **234**, 341-344.

23 G. Xing, N. Mathews, S. Sun, S. S. Lim, Y. M. Lam, M. Grätzel, S. Mhaisalkar, and T. C. Sum, Long-Range Balanced Electron and Hole-Transport Lengths In Organic-Inorganic $CH_3NH_3PbI_3$. *Science* 2013, **342**, 344-347.

24 S. Colella, E. Mosconi, P. Fedeli, A. Listorti, F. Gazza, F. Orlandi, P. Ferro, T. Besagni, A. Rizzo, G. Calestani, G. Gigli, F. De Angelis and R. Mosca, $MAPbI_{(3-x)}Cl_x$ Mixed Halide Perovskite for Hybrid Solar Cells: The role of Chloride as Dopant on the Transport and Structural Properties. *Chem. Mater.* 2013, **25**, 4613-4618.

25 C. Quarti, E. Mosconi, G. Grancini, J. M. Ball, M. L. Lee, H. J. Snaith, A. Petrozza. and F. De Angelis, The Raman spectrum of the $CH_3NH_3PbI_3$ hybrid perovskite: Interplay of theory and experiment. *J. Phys. Chem. Lett.* 2014, **5**, 279−284.

26 N. Onoda-Yamamuro, T. Matsuo and H. Suga, Calorimetric and IR Spectroscopic Studies of Phase Transitions in Methylammonium Trihalogenoplumbates (II). *J. Phys. Chem. Solids* 1990, **51**, 1383-1395.

27 T. Umebayashi, K. Asai, T. Kondo and A. Nakao, Electronic structures of lead iodide based low-dimensional crystals. *Phys. Rev. B*, 2003, **67**, 155405.

28 Y. H. Chang and C. H. Park, First-Principle Study of the Structural and the Electronic Properties of the Lead-Halide-Based Inorganic Perovskites $(CH_3NH_3)PbX_3$ and $CsPbX_3$ (X=Cl, Br, I). *J. Korean. Phys. Soc.* **2004**, *44*, 889-893.

29 E. Mosconi, A. Amat, Md. K. Nazeeruddin, M. Grätzel and F. De Angelis, First-Principles Modeling of Mixed Halide Organometal Perovskites for Photovoltaic Applications. *J. Phys. Chem. C* 2013, **117**, 13902-13913.

30 J. Even, L. Pedesseau, J. M. Jancu and C. Katan, Importance of Spin−Orbit Coupling in Hybrid Organic/Inorganic Perovskites for Photovoltaic Applications." *J. Phys. Chem. Lett.* 2013, **4**, 2999-3005.

31 J. Even, L. Pedesseau, J. M. Jancu and C. Katan, DFT and kp modeling of the phase transition of lead and tin halide perovskites for photovoltaic cells. Phys. Status Solidi rrl DOI: 10.1002/pssr.201308183.

32 F. Brivio, A. B. Walker and A. Walsh, Structural and electronic properties of hybrid perovskites for high-efficiency thin-film photovoltaics from first-principles. *Appl. Phys. Lett.* 2013, **1**, 042111.

33 L. Y. Huang and R. L. Lambrecht, Electronic band structure, phonons, and exciton binding energies of halide perovskites $CsSnCl_3$, $CsSnBr_3$, and $CsSnI_3$, *Phys. Rev. B* 2013, **88**, 165203/1-14.

34 R. Lindblad, D. Bi, B. W. Park, J. Oscarsson, M. Gorgoi, H. Siegbahn, M. Odelius, E. M. J. Johansson and H. Rensmo, The electronic structure of $TiO_2/CH_3NH_3PbI_3$ pervskite solar cell interfaces. *J. Phys. Chem. Lett.* 2014, **5**, 648-653.

35 R. Car and M. Parrinello, Unified Approach for Molecular Dynamics and Density-Functional Theory. *Physical Review Letters* ,1985, **55**, 2471–2474.

36 P. Giannozzi, S. Baroni, N. Bonini, M. Calandra, R. Car, C. Cavazzoni, D. Ceresoli, G. L. Chiarotti, M. Coccioni, I. Dabo, A. Dal Corso, S. de Gironcoli, S. Fabris, G. Fratesi, R. Gebauer, U. Gerstmann, C. Gougoussis, A. Kokalj, M. Lazzeri, L. Martin-Samos, N. Marzari, F. Mauri, R. Mazzarello, S. Paolini, A. Pasquarello, L. Paulatto, C. Sbraccia, S. Scandolo, G. Sclauzero, A. P. Seitsonen, A. Smogunov, P. Umari, and R. M. Wentzcovitch, QUANTUM ESPRESSO: a Modular and Open-Source Software Project for Quantum Simulations of Materials. *J. Phys: Condens. Matter* 2009, **21**, 395502.

37 J. P. Perdew, K. Burke and M. Ernzerhof, Generalized Gradient Approximation Made Simple. *Phys. Rev. B* 1996, **77**, 3865-3868.

38 D. Vanderbilt, Soft self-consistent pseudopotentials in a generalized eigenvalue formalism. *Phys. Rev. B*, 1990, *41*, 7892-7895.

39 M. P. Gaigeot, Theoretical spectroscopy of floppy peptides at room temperature. A DFTMD perspective: gas and aqueous phase. *Phys. Chem. Chem. Phys.* 2010, **12**, 3336-3359.

40 H. J. Monkhorst and J. D. Pack, Special Points for Brillouin-Zone Integrations. *Phys. Rev. B* 1976, **13**, 5188-5192.

41 B. Paci, G. Amoretti, G. Arduini, G. Ruani, S. Shinkai, T. Suzuki, F. Uguzzoli and R. Caciuffo, Vibrational spectrum of C_{60} in the p-tert-butylcalix[8]arene(1:1)C_{60} complex. *Phys. Rev. B* 1997, **55**, 5566-5569.

42 J. W. Handgraaf, E. J. Meijer and P. M. Gaigeot, Density-functional theory based molecular simulation study of liquid methanol. J. Chem. Phys. 2004, 121, 10111-10119.

43 F. De Angelis, S. Fantacci and R. Gebauer, Simulating Dye-Sensitized TiO2 Heterointerfaces in Explicit Solvent: Absorption Spectra, Energy Levels, and Dye desorption. *J. Phys. Chem. Lett.* 2011, **2**, 831-817.

44 A. Troisi, G. Orlandi and J. E. Anthony, Electronic Interactions and Thermal Disorder in Molecular Crystals Containing Cofacial Pentacene Units. *Chem. Mater.* 2005, **17**, 5024-5031.

45 A. Troisi and G. Orlandi, Dynamics of the Intermolecular Transfer Integral in Crystalline Organic Semiconductors. *J. Phys. Chem. A* 2006, **110**, 4065-4070.